

QCDF Amplitudes from $SU(3)$ Symmetries

Gilberto Tetlalmatzi-Xolocotzi^{a,b,*}

^a*Theoretische Physik 1, Naturwissenschaftlich-Technische Fakultät,
Universität Siegen, Walter-Flex-Strasse 3, D-57068 Siegen, Germany.*

^b*Université Paris-Saclay, CNRS/IN2P3, IJCLab, 91405 Orsay, France*

E-mail: gtx@physik.uni-siegen.de, huber@physik.uni-siegen.de

We determine the potential size of weak annihilation topologies contributing to the processes of B mesons decaying into pairs of pseudoscalar light mesons. Our purely phenomenological approach, is based on a fit to experimental data and assumes exact $SU(3)$ flavour symmetry.

*8th Symposium on Prospects in the Physics of Discrete Symmetries (DISCRETE 2022)
7-11 November, 2022
Baden-Baden, Germany*

*Speaker

1. Introduction

The decays of B mesons into charmless non-leptonic final states are useful for multiple reasons, for instance they allow to test the CKM mechanism and to probe for CP violation.

Different first principle theoretical techniques have been introduced to address non-leptonic B meson decays. This includes for instance PQCD [1], QCD-Factorization (QCDF) [2–4] and methods based on light flavour symmetries [5]. Unfortunately, in general, these computations entail contributions with big uncertainties or which cannot be determined by applying our current theoretical tools. QCDF is a powerful formalism and allows to disentangle short and long distance contributions in the heavy quark limit. Currently at the leading power in Λ_{QCD}/m_b , QCDF allows to perform calculations up to NNLO in the α_s expansion [6–12]. However, beyond the leading terms in Λ_{QCD}/m_b the uncertainties are large and spoil the precision achieved at the leading order. This includes for instance the so-called annihilation topologies which are non-factorizable and which lead to end-point singular integrals of the Light-Cone-Distribution Amplitudes (LCDA) of the final state mesons.

Here we present an approach to determine the potential size of the non-factorizable contributions appearing in QCDF for the processes $B_q \rightarrow PP$, where B_q is either a B^- , \bar{B}_d^0 or a \bar{B}_s^0 meson and P represents a pseudoscalar light meson. Our approach is phenomenological and makes use of experimental data. We take advantage of the relationship between different parameterizations of the decay amplitudes as well as of the $SU(3)$ -flavour symmetry [13]. In the subsequent sections we will introduce different options for the parameterizations of the amplitudes of the relevant decay processes: the Topological, the $SU(3)$ -Irreducible and the QCDF decompositions. In addition we will also provide the set of equations that allow to translate one description into another. Then, we will perform a χ^2 -fit to the $SU(3)$ -Irreducible amplitudes and we will map these results into the QCDF amplitudes. This will allow us to finally determine the potential size of the annihilation contributions as dictated by the state of the art experimental data.

2. Topological and $SU(3)$ -Irreducible decomposition of non-leptonic decay amplitudes for $B_q \rightarrow PP$ processes

Based on the CKM structure, we consider the following decomposition of the physical amplitudes for $B_q \rightarrow PP$ processes

$$\mathcal{A} = i \frac{G_F}{\sqrt{2}} \left[\mathcal{T} + \mathcal{P} \right]. \quad (1)$$

where \mathcal{T} and \mathcal{P} are characterized by the CKM factors $\lambda_u^{(q)}$ and $\lambda_t^{(q)}$ respectively, for

$$\lambda_p^{(q)} = V_{pb} V_{pq}^* \quad (2)$$

with $q = d, s$.

The contributions \mathcal{T} and \mathcal{P} can be parameterized in different ways. In the subsequent discussion we will focus on the sector \mathcal{T} , but an analogous treatment can be given to the \mathcal{P} sector. Thus, the Topological decomposition of \mathcal{T} is [14]

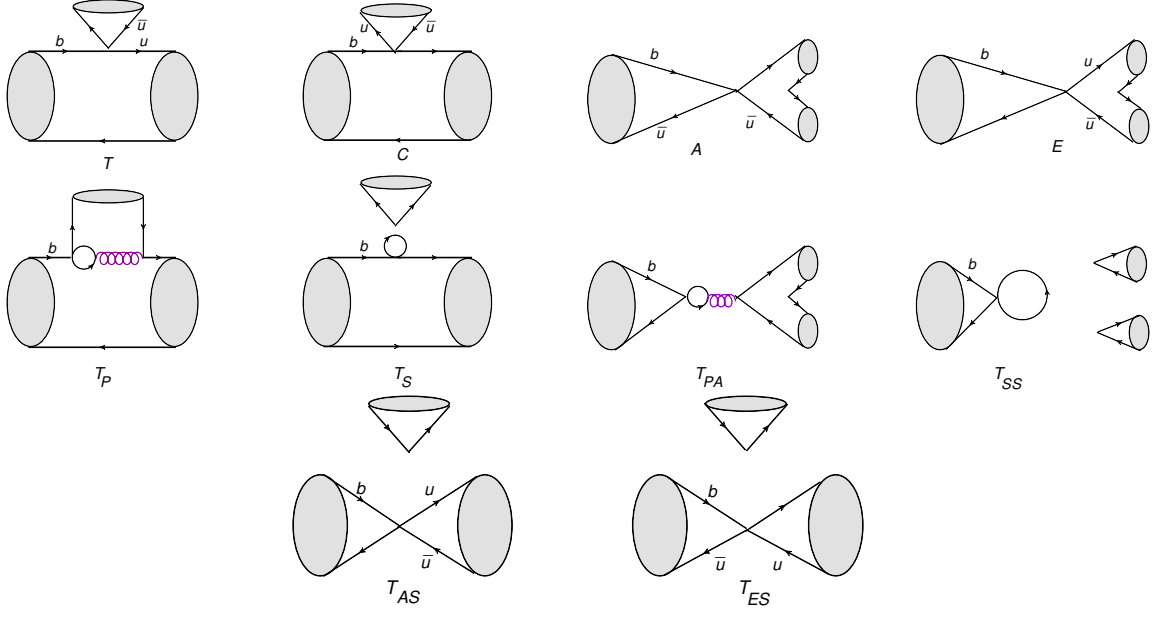


Figure 1: Diagrammatic representation of the tree-like topological amplitudes in Eq. (3).

$$\begin{aligned}
 \mathcal{T}^{TDA} = & T B_i(M)_j \bar{H}_k^{jl} (M)_l^k + C B_i(M)_j \bar{H}_k^{lj} (M)_l^k + A B_i \bar{H}_j^{il} (M)_k^j (M)_l^k \\
 & + E B_i \bar{H}_j^{li} (M)_k^j (M)_l^k + T_{ES} B_i \bar{H}_l^{ij} (M)_j^l (M)_k^k + T_{AS} B_i \bar{H}_l^{ji} (M)_j^l (M)_k^k \\
 & + T_S B_i(M)_j \bar{H}_l^{lj} (M)_k^k + T_{PA} B_i \bar{H}_l^{li} (M)_k^j (M)_j^k + T_P B_i(M)_j (M)_k^j \bar{H}_l^{lk} \\
 & + T_{SS} B_i \bar{H}_l^{li} (M)_j^j (M)_k^k.
 \end{aligned} \tag{3}$$

Where the initial states are organized in a $SU(3)$ triplet $B_i = (B^-, \bar{B}_d^0, \bar{B}_s^0)$. Analogously, the final states are included inside the light-meson matrix $(M)_j^i$ which is the result of a $SU(3)$ octet plus a singlet and has the structure

$$M = \begin{pmatrix} \frac{\pi^0}{\sqrt{2}} + \frac{\eta_q}{\sqrt{2}} + \frac{\eta'_q}{\sqrt{2}} & \pi^- & K^- \\ \pi^+ & -\frac{\pi^0}{\sqrt{2}} + \frac{\eta_q}{\sqrt{2}} + \frac{\eta'_q}{\sqrt{2}} & \bar{K}^0 \\ K^+ & K^0 & \eta_s + \eta'_s \end{pmatrix}. \tag{4}$$

The non-zero components of the flavour objects \bar{H} are

$$\begin{aligned}
 \bar{H}_1^{12} &= \lambda_u^{(d)}, & \bar{H}_1^{13} &= \lambda_u^{(s)}, \\
 \bar{H}^2 &= \lambda_u^{(d)}, & \bar{H}^3 &= \lambda_u^{(s)}.
 \end{aligned} \tag{5}$$

In the Topological decomposition each term in Eq. (3) is associated with a topology as indicated in Fig. 1.

Alternatively, we can express the tensor \bar{H}_k^{ji} in terms of irreducible representations of $SU(3)$ as follows

$$\bar{H}_k^{ij} = \frac{1}{8}(\bar{H}_{15})_k^{ij} + \frac{1}{4}(\bar{H}_6)_k^{ij} - \frac{1}{8}(\bar{H}_3)^i \delta_k^j + \frac{3}{8}(\bar{H}_{3'})^j \delta_k^i. \quad (6)$$

We can then re-write Eq. (3) as [14]

$$\begin{aligned} \mathcal{T}^{IRA} = & A_3^T B_i(\bar{H}_3)^i(M)_k^j(M)_j^k + C_3^T B_i(M)_j^i(M)_k^j(\bar{H}_3)^k + B_3^T B_i(\bar{H}_3)^i(M)_k^j(M)_j^k \\ & + D_3^T B_i(M)_j^i(\bar{H}_3)^j(M)_k^k + A_6^T B_i(\bar{H}_6)_k^{ij}(M)_j^l(M)_l^k + C_6^T B_i(M)_j^i(\bar{H}_6)_k^{jl}(M)_l^k \\ & + B_6^T B_i(\bar{H}_6)_k^{ij}(M)_j^k(M)_l^l + A_{15}^T B_i(\bar{H}_{15})_k^{ij}(M)_j^l(M)_l^k + C_{15}^T B_i(M)_j^i(\bar{H}_{15})_l^{jk}(M)_k^l \\ & + B_{15}^T B_i(\bar{H}_{15})_k^{ij}(M)_j^k(M)_l^l. \end{aligned} \quad (7)$$

with

$$\begin{aligned} (\bar{H}_3)^2 = \lambda_u^{(d)}, \quad (\bar{H}_6)_1^{12} = -(\bar{H}_6)_1^{21} = (\bar{H}_6)_3^{23} = -(\bar{H}_6)_3^{32} = \lambda_u^{(d)}, \\ 2(\bar{H}_{15})_1^{12} = 2(\bar{H}_{15})_1^{21} = -3(\bar{H}_{15})_2^{22} = -6(\bar{H}_{15})_3^{23} = -6(\bar{H}_{15})_3^{32} = 6\lambda_u^{(d)}, \end{aligned} \quad (8)$$

and

$$\begin{aligned} (\bar{H}_3)^3 = \lambda_u^{(s)}, \quad (\bar{H}_6)_1^{13} = -(\bar{H}_6)_1^{31} = (\bar{H}_6)_3^{32} = -(\bar{H}_6)_3^{23} = \lambda_u^{(s)}, \\ 2(\bar{H}_{15})_1^{13} = 2(\bar{H}_{15})_1^{31} = -3(\bar{H}_{15})_3^{33} = -6(\bar{H}_{15})_3^{32} = -6(\bar{H}_{15})_3^{23} = 6\lambda_u^{(s)}. \end{aligned} \quad (9)$$

Once the physical amplitudes are computed, the component A_6^T appears always in the combinations $C_6^T - A_6^T$ and $B_6^T + A_6^T$ and consequently it can always be absorbed according to the following rules,

$$C_6^T - A_6^T \rightarrow C_6^T, \quad B_6^T + A_6^T \rightarrow B_6^T, \quad (10)$$

and similarly for the corresponding penguin amplitudes.

The Topological and the $SU(3)$ -Irreducible parameterizations are related each other according to the following equations

$$\begin{aligned} A_3^T &= -\frac{A}{8} + \frac{3E}{8} + T_{PA}, & B_3^T &= T_{SS} + \frac{3T_{AS} - T_{ES}}{8}, \\ C_3^T &= \frac{1}{8}(3A - C - E + 3T) + T_P, & D_3^T &= T_S + \frac{1}{8}(3C - T_{AS} + 3T_{ES} - T), \\ A_6^T &= \frac{1}{4}(A - E), & B_6^T &= \frac{1}{4}(T_{ES} - T_{AS}), \\ C_6^T &= \frac{1}{4}(-C + T), & A_{15}^T &= \frac{A + E}{8}, \\ B_{15}^T &= \frac{T_{ES} + T_{AS}}{8}, & C_{15}^T &= \frac{C + T}{8}. \end{aligned} \quad (11)$$

3. Phenomenological determination of the amplitudes

To assess the set of values for the $SU(3)$ -Irreducible amplitudes compatible with experimental data a χ^2 -fit is performed. Our analysis includes branching fractions and CP asymmetries for non leptonic B meson decays defined respectively as

$$\mathcal{B}(\bar{B} \rightarrow \bar{f}) = \frac{1}{2}\tau_B \left[\Gamma(\bar{B} \rightarrow \bar{f}) + \Gamma(B \rightarrow f) \right] \quad \text{and} \quad \mathcal{A}_{\text{CP}}(\bar{B} \rightarrow \bar{f}) = \frac{\Gamma(\bar{B} \rightarrow \bar{f}) - \Gamma(B \rightarrow f)}{\Gamma(\bar{B} \rightarrow \bar{f}) + \Gamma(B \rightarrow f)}, \quad (12)$$

where the decay width is then evaluated as

$$\Gamma(\bar{B} \rightarrow f) = \frac{S}{16\pi M_B} |\mathcal{A}_{B \rightarrow f}|^2. \quad (13)$$

Our best fit point for the $SU(3)$ -Irreducible amplitudes in \mathcal{T}^{IRA} is [13]

$$\begin{aligned} |A_3^T| &= 0.029, & \delta_{A_3^T} &= -3.083, & |C_3^T| &= 0.258, & \delta_{C_3^T} &= -0.105, \\ |C_6^T| &= 0.235, & \delta_{C_6^T} &= -0.079, & |A_{15}^T| &= 0.029, & \delta_{A_{15}^T} &= -3.083, \\ |C_{15}^T| &= 0.151, & \delta_{C_{15}^T} &= 0.061, & |B_3^T| &= 0.034, & \delta_{B_3^T} &= 3.087, \\ |B_6^T| &= 0.033, & \delta_{B_6^T} &= -0.286, & |B_{15}^T| &= 0.008, & \delta_{B_{15}^T} &= -1.892, \\ |D_3^T| &= 0.055, & \delta_{D_3^T} &= 2.942, & & & & \end{aligned} \quad (14)$$

and for the corresponding amplitudes in \mathcal{P}^{IRA} we get

$$\begin{aligned} |A_3^P| &= 0.014, & \delta_{A_3^P} &= -1.328, & |C_6^P| &= 0.145, & \delta_{C_6^P} &= -2.881, \\ |A_{15}^P| &= 0.003, & \delta_{A_{15}^P} &= 2.234, & |C_{15}^P| &= 0.003, & \delta_{C_{15}^P} &= -0.608, \\ |B_3^P| &= 0.043, & \delta_{B_3^P} &= 2.367, & |B_6^P| &= 0.099, & \delta_{B_6^P} &= 0.353, \\ |B_{15}^P| &= 0.031, & \delta_{B_{15}^P} &= -0.690, & |D_3^P| &= 0.030, & \delta_{D_3^P} &= 0.477, \\ |C_3^P| &= 0.008, & \theta_{FKS} &= 0.628. & & & & \end{aligned} \quad (15)$$

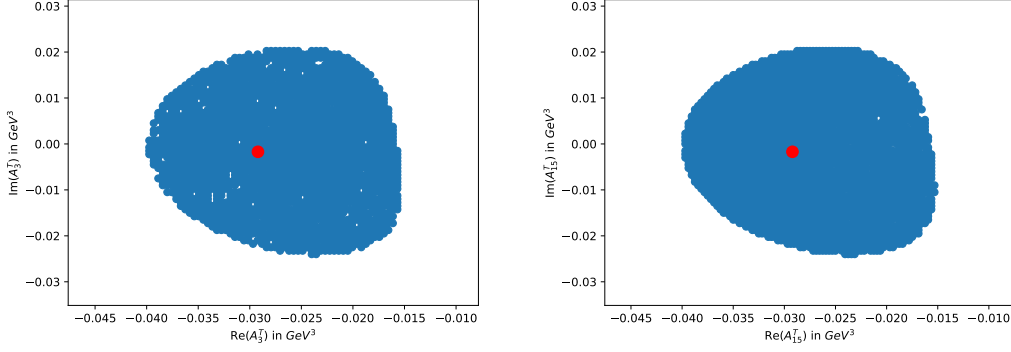
where the modulus are given in units of GeV^3 . The phase θ_{FKS} refers to the η meson mixing angle in the Feldmann–Kroll–Stech scheme [15]. Our minimum point leads to the following χ^2 per degree of freedom value

$$\chi^2/d.o.f. = 0.851. \quad (16)$$

For the determination of the confidence intervals of our $SU(3)$ parameters, we perform a likelihood ratio test applying Wilk's theorem. We find convenient to study the allowed regions in the space expanded by the real and the imaginary components of each one of the $SU(3)$ -Irreducible amplitudes at the 68% confidence level. Examples of the regions obtained are shown in Fig. 2, moreover in Table 1 we present our determinations for the branching fractions for some non leptonic B meson decay channels into pairs of pseudoscalar particles.

4. Amplitudes in QCD Factorization

The calculation of the amplitude for $B \rightarrow PP$ in QCDF can be obtained by applying the general formula [17]

Figure 2: $SU(3)$ confidence regions.

| Channel | Branching ratio in units of 10^{-6} | | Channel | Branching ratio in units of 10^{-6} | |
|---------------------------------------|--|-------------------------|-------------------------------------|--|---------------------------|
| | Experimental [16] | Theoretical | | Experimental [16] | Theoretical |
| $B^- \rightarrow \pi^0 \pi^-$ | 5.5 ± 0.4 | $6.04^{+2.42}_{-2.51}$ | $B^- \rightarrow \eta \pi^-$ | 4.02 ± 0.27 | $3.80^{+1.25}_{-1.55}$ |
| $B^- \rightarrow K^0 K^-$ | 1.31 ± 0.17 | $1.36^{+0.17}_{-0.16}$ | $B^- \rightarrow \eta' \pi^-$ | 2.7 ± 0.9 | $3.55^{+4.49}_{-1.67}$ |
| $\bar{B}^0 \rightarrow \pi^+ \pi^-$ | 5.12 ± 0.19 | $6.31^{+0.61}_{-0.50}$ | $\bar{B}^0 \rightarrow \eta \pi^0$ | 0.41 ± 0.17 | $0.41^{+8.90}_{-4.08}$ |
| $\bar{B}^0 \rightarrow \pi^0 \pi^0$ | 1.59 ± 0.26 | $1.01^{+1.30}_{-0.51}$ | $\bar{B}^0 \rightarrow \eta' \pi^0$ | 1.2 ± 0.6 | $1.20^{+3.62}_{-1.19}$ |
| $\bar{B}^0 \rightarrow K^+ K^-$ | 0.078 ± 0.015 | $0.13^{+0.08}_{-0.07}$ | $\bar{B}_s \rightarrow \eta K^0$ | Not available | $0.13^{+0.11}_{-0.08}$ |
| $\bar{B}^0 \rightarrow K^0 \bar{K}^0$ | 1.21 ± 0.16 | $1.13^{+0.83}_{-0.91}$ | $\bar{B}_s \rightarrow \eta' K^0$ | Not available | $6.65^{+1.48}_{-1.65}$ |
| $\bar{B}_s \rightarrow \pi^- K^+$ | 5.8 ± 0.7 | $7.75^{+0.63}_{-0.09}$ | $B^- \rightarrow \eta K^-$ | 2.4 ± 0.4 | $2.34^{+1.39}_{-1.67}$ |
| $B^- \rightarrow \pi^0 K^-$ | 12.9 ± 0.5 | $12.78^{+1.75}_{-1.94}$ | $B^- \rightarrow \eta' K^-$ | 70.4 ± 2.5 | $70.82^{+11.16}_{-11.53}$ |
| $B^- \rightarrow \pi^- \bar{K}^0$ | 23.7 ± 0.8 | $23.85^{+2.23}_{-2.31}$ | $\bar{B}^0 \rightarrow \eta K^0$ | 1.23 ± 0.27 | $1.38^{+1.15}_{-0.36}$ |
| $\bar{B}^0 \rightarrow \pi^+ K^-$ | 19.6 ± 0.5 | $19.47^{+1.72}_{-2.24}$ | $\bar{B}^0 \rightarrow \eta' K^0$ | 6.6 ± 0.4 | $6.65^{+1.48}_{-1.65}$ |

Table 1: Experimental input and fit results for CP-averaged branching fractions.

$$\begin{aligned}
\mathcal{A}^{\text{QCDF}} = & i \frac{G_F}{\sqrt{2}} \sum_{p=u,c} A_{M_1 M_2} \left\{ BM_1 \left(\alpha_1 \delta_{pu} \hat{U} + \alpha_4^p \hat{I} + \alpha_{4,EW}^p \hat{Q} \right) M_2 \Lambda_p \right. \\
& + BM_1 \Lambda_p \cdot \text{Tr} \left[\left(\alpha_2 \delta_{pu} \hat{U} + \alpha_3^p \hat{I} + \alpha_{3,EW}^p \hat{Q} \right) M_2 \right] \\
& + B \left(\beta_2 \delta_{pu} \hat{U} + \beta_3^p \hat{I} + \beta_{3,EW}^p \hat{Q} \right) M_1 M_2 \Lambda_p \\
& + B \Lambda_p \cdot \text{Tr} \left[\left(\beta_1 \delta_{pu} \hat{U} + \beta_4^p \hat{I} + b_{4,EW}^p \hat{Q} \right) M_1 M_2 \right] \\
& + B \left(\beta_{S2} \delta_{pu} \hat{U} + \beta_{S3}^p \hat{I} + \beta_{S3,EW}^p \hat{Q} \right) M_1 \Lambda_p \cdot \text{Tr} M_2 \\
& \left. + B \Lambda_p \cdot \text{Tr} \left[\left(\beta_{S1} \delta_{pu} \hat{U} + \beta_{S4}^p \hat{I} + b_{S4,EW}^p \hat{Q} \right) M_1 \right] \cdot \text{Tr} M_2 \right\}, \quad (17)
\end{aligned}$$

where

$$\Lambda_P = \begin{pmatrix} 0 \\ \lambda_P^{(d)} \\ \lambda_P^{(s)} \end{pmatrix}, \quad \hat{U} = \begin{pmatrix} 1 & 0 & 0 \\ 0 & 0 & 0 \\ 0 & 0 & 0 \end{pmatrix},$$

$$\hat{Q} = \frac{3}{2}\hat{Q} = \begin{pmatrix} 1 & 0 & 0 \\ 0 & -\frac{1}{2} & 0 \\ 0 & 0 & -\frac{1}{2} \end{pmatrix}, \quad \hat{I} = \begin{pmatrix} 1 & 0 & 0 \\ 0 & 1 & 0 \\ 0 & 0 & 1 \end{pmatrix}, \quad (18)$$

and the $SU(3)$ triplet B and $SU(3)$ octet M coincide with the ones introduced in section 2.

The parameterization of the physical amplitude in Eq. (17) can be related to the Topological decomposition by using

$$\hat{Q} = \frac{3}{2}\hat{U} - \frac{1}{2}\hat{I} \quad \text{and} \quad \Lambda_t = -\Lambda_u - \Lambda_c. \quad (19)$$

Then, by expressing the matrices in Eqs. (18) in terms of components we find

$$U_k^i(\Lambda_u)^j = \bar{H}_k^{ij}. \quad (20)$$

For completeness we also write the corresponding transformation for the flavour structures \tilde{H}_k^{ij} and \tilde{H}^i appearing in the \mathcal{P} sector

$$U_k^i(\Lambda_t)^j = \tilde{H}_k^{ij}, \quad (\Lambda_t)^i = \tilde{H}^i. \quad (21)$$

The set of Eqs. (20) and (21) are the basic pieces required to transform the Topological description into the QCDF one. The general solution for the transformation equations can be found in [13]. However, these expressions can be simplified by taking into account the following NLO results [17]

$$\alpha_3^u = \alpha_3^c = \alpha_3, \quad \alpha_{3,EW}^u = \alpha_{3,EW}^c = \alpha_{3,EW}, \quad \beta_i^u = \beta_i^c = \beta_i, \quad b_i^u = b_i^c = b_i. \quad (22)$$

In addition, considering that at NLO the amplitudes $\alpha_{4,EW}^P$ are at the permille level, the differences $|\alpha_{4,EW}^c - \alpha_{4,EW}^u|$ can be at most $\mathcal{O}(10^{-3})$. Analogously for α_4^P the magnitudes are about 10%, and the differences $|\alpha_4^c - \alpha_4^u|$ are about 2%. Accounting for all these approximations we can obtain the following set of equations relating the Topological and the QCDF parameterizations

$$\begin{aligned} T &= A_{M_1 M_2} \alpha_1, & C &= A_{M_1 M_2} \alpha_2, & E &= A_{M_1 M_2} \beta_1, \\ A &= A_{M_1 M_2} \beta_2, & T_{AS} &= A_{M_1 M_2} \beta_{S1}, & T_{ES} &= A_{M_1 M_2} \beta_{S2}, \end{aligned}$$

$$\begin{aligned} S &= -A_{M_1 M_2} \left[\alpha_3 + \beta_{S3} - \frac{\alpha_{3,EW}}{2} - \frac{\beta_{S3,EW}}{2} \right], \\ P &= -A_{M_1 M_2} \left[\alpha_4^c + \beta_3 - \frac{\alpha_{4,EW}^c}{2} - \frac{\beta_{3,EW}}{2} \right], \end{aligned}$$

$$\begin{aligned}
 P_A &= -A_{M_1 M_2} \left(\beta_4 - \frac{b_{4,EW}}{2} \right), & P_{SS} &= -A_{M_1 M_2} \left(\beta_{S4} - \frac{b_{S4,EW}}{2} \right), \\
 P_C &= -\frac{3}{2} A_{M_1 M_2} \alpha_{3,EW}, & P_T &= -\frac{3}{2} A_{M_1 M_2} \alpha_{4,EW}^c, \\
 P_{TA} &= -\frac{3}{2} A_{M_1 M_2} \beta_{3,EW}, & P_{TE} &= -\frac{3}{2} A_{M_1 M_2} b_{4,EW}, \\
 P_{AS} &= -\frac{3}{2} A_{M_1 M_2} b_{S4,EW}, & P_{ES} &= -\frac{3}{2} A_{M_1 M_2} \beta_{S3,EW}, \\
 T_{PA} &= 0, & T_{SS} &= 0, & T_S &= 0, & |T_P| &< 0.02. \quad (23)
 \end{aligned}$$

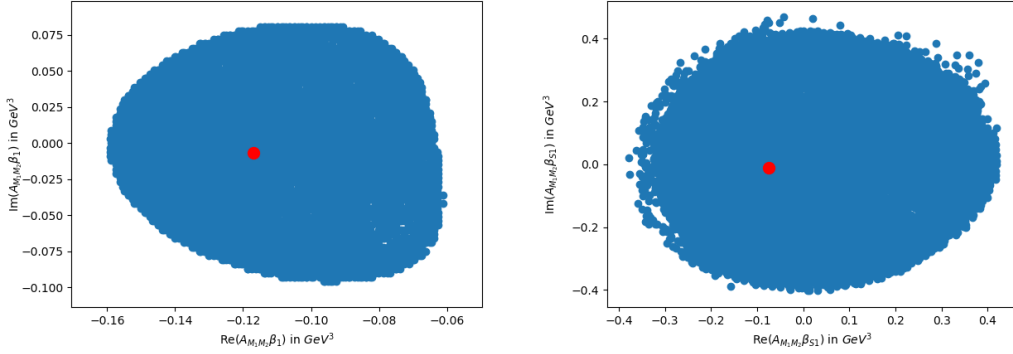


Figure 3: QCDF confidence regions.

By taking advantage of the transformation equations in Eq. (11), we can then translate the results of our χ^2 -fit as described in Sec. 3 into the corresponding values for the different QCDF amplitudes α_j , β_j and b_j . Here we present the confidence regions for β_1 and β_{S1} in Fig. 3. These are two examples of the results we were aiming for. We can see how the real and imaginary components of the annihilation amplitudes β_1 can be in the ballpark of 10% and being as sizeable as 40% for the singlet contributions β_{S1} . The large values for this latter contribution arises from the fact that the constraints on these quantities come mostly from the channels involving η mesons in the final states. Unfortunately, currently the observables associated with these channels suffer from large uncertainties.

5. Conclusions

The aim of the present work was to determine the potential size of the regions for the weak annihilation amplitudes in QCDF following a data-driven approach. To fulfill this goal we have established a set of transformation rules between the Topological and the QCDF decompositions. We have then performed a global fit to the $SU(3)$ -Irreducible amplitudes with a few additional mild assumptions. Then, assuming flavour $SU(3)$ to be unbroken, we have exploited the connection between the QCDF and the $SU(3)$ -Irreducible/Topological descriptions to translate the fit results into 1σ confidence regions of the real and imaginary parts of the QCDF amplitudes.

Our results indicate that the size of some of the annihilation amplitudes in the parameterization of QCDF get constrained very well around or below 10% whereas others can take values up to

$\sim 40\%$ which holds for those involved in channels with η mesons. While the confidence regions obtained from the fit are in many cases still sizeable they can be regarded as upper bounds, and provide valuable information on non-perturbative input parameters useful in future phenomenological studies on two-body charmless non-leptonic $B_{(s)}$ decays. Moreover, with improved experimental data the potential size of these physical contributions will get further reduced.

Acknowledgements

We thank Tobias Huber for his input on this report. This project has received funding from the European Union's Horizon 2020 research and innovation programme under the Marie Skłodowska-Curie grant agreement No 945422. This research has been supported by the Deutsche Forschungsgemeinschaft (DFG, German Research Foundation) under grant 396021762 - TRR 257.

References

- [1] Y. Y. Keum, H. n. Li and A. I. Sanda, Phys. Lett. B **504** (2001), 6-14 doi:10.1016/S0370-2693(01)00247-7 [arXiv:hep-ph/0004004 [hep-ph]].
- [2] M. Beneke, G. Buchalla, M. Neubert and C. T. Sachrajda, Phys. Rev. Lett. **83** (1999), 1914-1917 doi:10.1103/PhysRevLett.83.1914 [arXiv:hep-ph/9905312 [hep-ph]].
- [3] M. Beneke, G. Buchalla, M. Neubert and C. T. Sachrajda, Nucl. Phys. B **591** (2000), 313-418 doi:10.1016/S0550-3213(00)00559-9 [arXiv:hep-ph/0006124 [hep-ph]].
- [4] M. Beneke, G. Buchalla, M. Neubert and C. T. Sachrajda, Nucl. Phys. B **606** (2001), 245-321 doi:10.1016/S0550-3213(01)00251-6 [arXiv:hep-ph/0104110 [hep-ph]].
- [5] D. Zeppenfeld, Z. Phys. C **8** (1981), 77 doi:10.1007/BF01429835
- [6] G. Bell, Nucl. Phys. B **795** (2008), 1-26 doi:10.1016/j.nuclphysb.2007.09.006 [arXiv:0705.3127 [hep-ph]].
- [7] G. Bell, Nucl. Phys. B **822** (2009), 172-200 doi:10.1016/j.nuclphysb.2009.07.012 [arXiv:0902.1915 [hep-ph]].
- [8] G. Bell and V. Pilipp, Phys. Rev. D **80** (2009), 054024 doi:10.1103/PhysRevD.80.054024 [arXiv:0907.1016 [hep-ph]].
- [9] M. Beneke, T. Huber and X. Q. Li, Nucl. Phys. B **832** (2010), 109-151 doi:10.1016/j.nuclphysb.2010.02.002 [arXiv:0911.3655 [hep-ph]].
- [10] G. Bell and T. Huber, JHEP **12** (2014), 129 doi:10.1007/JHEP12(2014)129 [arXiv:1410.2804 [hep-ph]].
- [11] G. Bell, M. Beneke, T. Huber and X. Q. Li, Phys. Lett. B **750** (2015), 348-355 doi:10.1016/j.physletb.2015.09.037 [arXiv:1507.03700 [hep-ph]].

- [12] G. Bell, M. Beneke, T. Huber and X. Q. Li, *JHEP* **04** (2020), 055
doi:10.1007/JHEP04(2020)055 [arXiv:2002.03262 [hep-ph]].
- [13] T. Huber and G. Tetlalmatzi-Xolocotzi, *Eur. Phys. J. C* **82** (2022) no.3, 210
doi:10.1140/epjc/s10052-022-10068-8 [arXiv:2111.06418 [hep-ph]].
- [14] X. G. He and W. Wang, *Chin. Phys. C* **42** (2018) no.10, 103108 doi:10.1088/1674-1137/42/10/103108 [arXiv:1803.04227 [hep-ph]].
- [15] T. Feldmann, P. Kroll and B. Stech, *Phys. Rev. D* **58** (1998), 114006
doi:10.1103/PhysRevD.58.114006 [arXiv:hep-ph/9802409 [hep-ph]].
- [16] P. A. Zyla *et al.* [Particle Data Group], *PTEP* **2020** (2020) no.8, 083C01
doi:10.1093/ptep/ptaa104
- [17] M. Beneke and M. Neubert, *Nucl. Phys. B* **675** (2003), 333-415
doi:10.1016/j.nuclphysb.2003.09.026 [arXiv:hep-ph/0308039 [hep-ph]].